Advances in Science and Technology Research Journal

Advances in Science and Technology Research Journal 2023, 17(5), 48–55
https://doi.org/10.12913/22998624/171020
ISSN 2299-8624, License CC-BY 4.0

Received: 2023.07.17
Accepted: 2023.09.14
Published: 2023.10.20

Microstructure and Mechanical Properties of AISI 1106 /AISI 1045 Steels Drawn Arc Stud Welded Joints

Samer Jasim Mahmood Algodi[1*], Abdulhakeem Amer Salman[1], Ali H. Al-Helli[1]

[1] Department of Mechanical Engineering, Collage of Engineering, Al-Nahrain University, Jadriya, Baghdad, Iraq

* Corresponding author's e-mail: samer.j.mahmoud@nahrainuniv.edu.iq

ABSTRACT

Arc stud welding process was used to join a fully threaded low carbon steel AISI 1106 stud to medium carbon steel AISI 1045 plate, the effects of welding current 200, 400 A and the welding time 0.1 to 0.6 step 0.1 s on the microstructure and mechanical properties were investigated, additional parameters of adding 0.1, 1 g SiC powder and applying nano carbon layer to the welding area also included. The results demonstrate that the preferred stud welding process parameters for this system was 400 A with 0.4 s welding current and time, respectively, which has a maximum tensile strength of 583 MPa. The joints fabricated with ash and nano carbon coated at preferred welding parameters showed a slight reduction in tensile strength. The fracture of the tensile test specimen consists of three failure modes including of interface fracture between stud and plate surface due to incomplete melting at low processing parameter, pullout fracture which is featured by a hole in the plate surface and fracture at the stud shank instead of the weldment interface or heat affected zone. The microstructure of the stud and plate are characterized by equiaxed grain of ferrite and pearlite with small amount of ferrite, respectively. The fusion zone consists of fine grain of ferrite and perlite. The hardness of the fusion zone was recording 132 HV which it slightly higher than the stud hardness 128 HV and lower than that of plate of 164 HV.

Keywords: arc stud welding, carbon steel, tensile strength, dissimilar welding.

INTRODUCTION

The drawn arc stud welding (DASW) process is a welding technique that is used for joining a metal stud shape or similar with various dimensions to a metal sheet or plate with different thickness. The process involves the same of the other arc welding principles including mechanical, electrical, and metallurgical [1, 2]. However, the process is distinguished by good welding quality with full joint and short welding time [3-5]. It is characterized by high local heat input to welding zone due to high current and presence of ceramic ferrule which protect the melt pool and hold metal vapor as a shielding gas with high cooling rate leading to small heat affected zone [6]. In general, stud welding is applied in different industries and production area such as steel structures, tank, pipe, steam boiler construction, automotive construction, underwater and shipbuilding etc. [7]. Arc stud welding can be divided into two main types, the arc stud welding process with ceramic ferrule and the short cycle arc stud welding process with or without shielding gas. And the capacitor discharge (CD) stud welding process without ferrule and shielding gas [8].

The operation of arc stud welding sequence is illustrated in Figure 1, the process starts with load the stud with ceramic ferrule into the chuck of the welding gun and positioned on the base plate surface. The gun then pushed against the base workpiece taking up the plunge. The trigger button is pressed to start a fully mechanized sequence including lifts up the stud for a defined distance. An initial welding arc is generated, the main welding current is passes through the electric path for a set of time, resulting in melting both the ends of the stud and the work piece underneath. When the

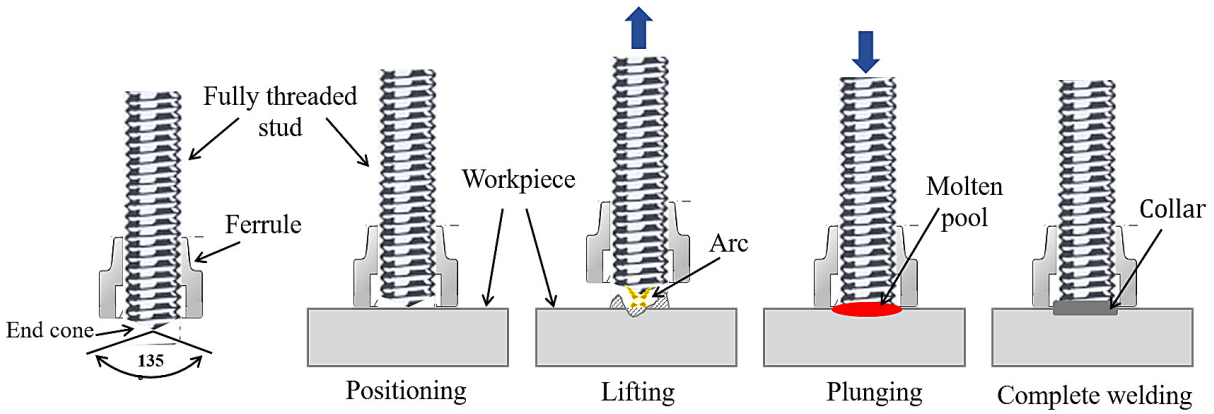

Fig. 1. Schematic of drawn arc stud welding process with ceramic ferrule, including positioning, lifting, plunging and complete welding

arc duration time is completed, the stud is plunged into the molten weld pool, and the current is cut off at the end of the weld cycle. Finally, the welding is completed and the weld molten pool is solidified and the gun is lifted off and with mechanically removing the ceramic ferrule [1, 9, 10].

The quality of the joint produce using arc stud welding is depended on different variables such as stud and base plate materials, welding current and time duration, plunge and lift distance. Several attempts have been made to understand the effects of welding parameters on the mechanical properties and microstructure of the arc stud weldments. For instance, NF Yilmaz et. al. [11] report that welding current and time must be selected correctly to obtain a high-performance welding joint. Hsu and Mumaw [12] investigate the weldability of different types of advanced high-strength steels using drawn arc stud welding. The weld quality and optimum welding parameter are depending on the steel types and thickness. Qian et.al. [13] carried out an experimental and numerical simulation of the Capacitor discharge stud welding of 20 carbon steel plate, the results showed that the microhardness of the weldments increased with an increase in the welding time and voltage.

The dissimilar welding process of different types of steel results in metallurgical difficulties including solidification cracks voids and brittle phases formation which may causes a reduction in the expected service life [14, 15]. The arc stud welding is successfully applied to join dissimilar materials including different grades of stainless steel and carbon steel for example, Abbas, E.N et.al. [16] investigate the arc stud welding of AISI 309 stainless steel to AISI 1020. Increase the current and welding time results in encourage the martensitic transformation of the carbon steel in the heat affected zone with increase the possibility of sigma phase formation in fusion zone, with increase the hardness at preferred parameters. Başyiğit, and Kurt [17] reported the increasing in tensile strength of arc stud welding of AISI 304 stainless steel /USN duplex stainless steel with welding arc voltage from 140 V to 180 V. Buranapunviwat, K. and Sojiphan [18] demonstrated that the welding time is mainly affected the power input of arc stud ASTM A36 steel joint, resulting in 80% welded area with the failure occurred in the stud flange instead of welded interface or heat affected zone at (25-30 μs).

A novel approach of adding micro/nano powder to welding zone proposed to produce a metal matrix composite within the fusion zone. For instance, Lin et. al. [19] investigates the microstructure and wear behaviour of SiC cladding layer on the SKD61 die steel using gas tungsten arc welding. Mohammad et. al. [20] studied the effects of include nano and micro SiC powder during dissimilar friction stir welding. Xie et. al. [21] applied mixed of TiO_2 and nano-SiC particles coated on the AZ31 magnesium alloy before TIG welding.

In this context, there is a requirement for optimization and improve the understanding the arc stud welding process. Therefore, the present paper focused on the characterization of microstructure and mechanical properties to provide a map of the arc stud welding process with ceramic ferrule of low carbon steel AISI 1106 stud / medium carbon steel AISI 1045 plate system as a function of welding current and time with the impact of adding alloying element of micro SiC particles to the welding and carbon nano layer to improve arc welding stability.

EXPERIMENTAL WORK

In the present work, a fully threaded low carbon steel AISI 1106 studs with dimension of 10 mm diameter, 80 mm length and the end cone angle of 135° were used to weld on 8 mm medium carbon steel AISI 1045 plate base material, the chemical composition of the stud and base material is performed using a Spectro analytical instrument presents in Table 1. The base metal is polished to a mirror finish, and then both stud and base plate were cleaned carefully with ethyl alcohol from contamination and dried with warm air before welding.

The arc stud welding with single use ceramic ferrules were performed on DABOTEK (DT1000) welding machine, different welding current 200 and 400 A with welding time of 0.1 to 0.6 step 0.1 s were employed for each current to perform the welding. The rest of process parameters such as the plunge and lift were kept constant at 1.5 mm and 4 mm, respectively. Three welding joints then performed with the preferred parameters including adding SiC with size about 45 µm of 0.1 and 1 g to the welding area inside the ferrules, adding ash layer and carbon nano layer was performed using Q150 Plus Coater.

The metallurgical analyses of the welding were performed using Optical microscope model Olympus microscope equipped with a digital camera. The cross section of the welding was cute using cutting machine and the sectioned samples mounted, grinded, polished, washed and etched with Nital (2 ml HNO_3 and 98 ml ethyl alcohols).

The welding assessment was done according to the EN ISO 14555 [22] standard, which include, visual inspection which can exclude the insufficient welding condition samples. The tensile strength of the arc welding was investigated using GUNT-WP310 Materials testing, 50kN machine, the applied loading speed was set as 1 mm/min up to the fracture taken place. A suitable tension device was designed and prepared for the stud welding tensile test, which consists of a special top grip that assemble the nut to screw on the threaded stud on a recessed ledge inside of the bored out tube, and the bottom grip that is holding the welded workpiece plate as illustrated in Figure 2. Each test was repeated at least 3 times to determine the average. The Vicker's hardness test was performed in the area of the cross section stud weldments across the base metal BM, heat affected zone HAZ, and fusion zone FZ with 300 g and 15 s dwell time.

RESULTS AND DISCUSSION

Tensile strength and fracture mode

Figures 3 shows the tensile strength of the arc stud welding as a function of increasing of welding currents 200, 400 A and welding times 0.1 to 0.6 step 0.1 sec. Figure 3a present the mean tensile strength of the weldments processed at 200 A and different welding times. The minimum tensile strength recorded at 0.1 and 0.2 sec, which is about 258 MPa and 263 MPa, respectively. This is probably due to the incomplete melting and alloying of the threaded stud with the flat workpiece as a result of short welding time. The tensile strength increased to reach 466 MPa at 0.4 sec, then decrease slightly to 448 MPa at 0.6 sec.

Figure 3b presents the tensile strength of the samples processed at 400 A and different welding times 0.1, 0.2, 0.3, 0.4, 0.5, 0.6 sec. The mean

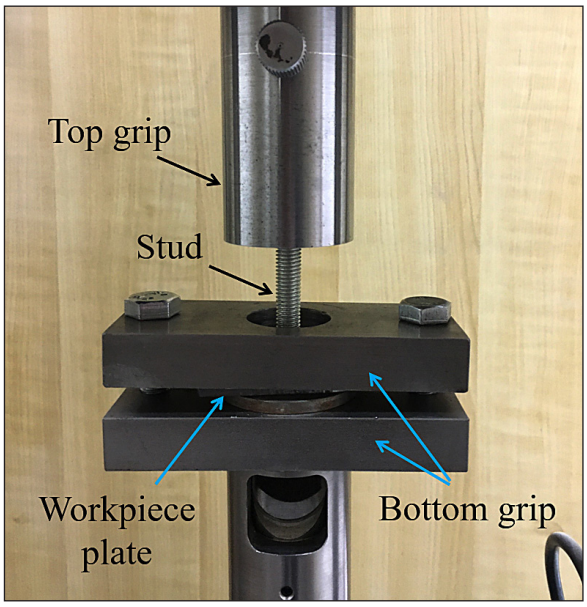

Fig. 2. Gripping Device for tensile test

Table 1. The chemical composition of the stud and plate

Elements %	C	Si	Mn	P	S	Cr	Ni	Cu	Fe
stud	0.0563	0.112	0.374	0.0202	0.0341	0.0135	0.0093	0.0101	Bal.
plate	0.4511	0.158	0.601	0.0190	0.0434	0.0436	0.0309	0.0011	Bal.

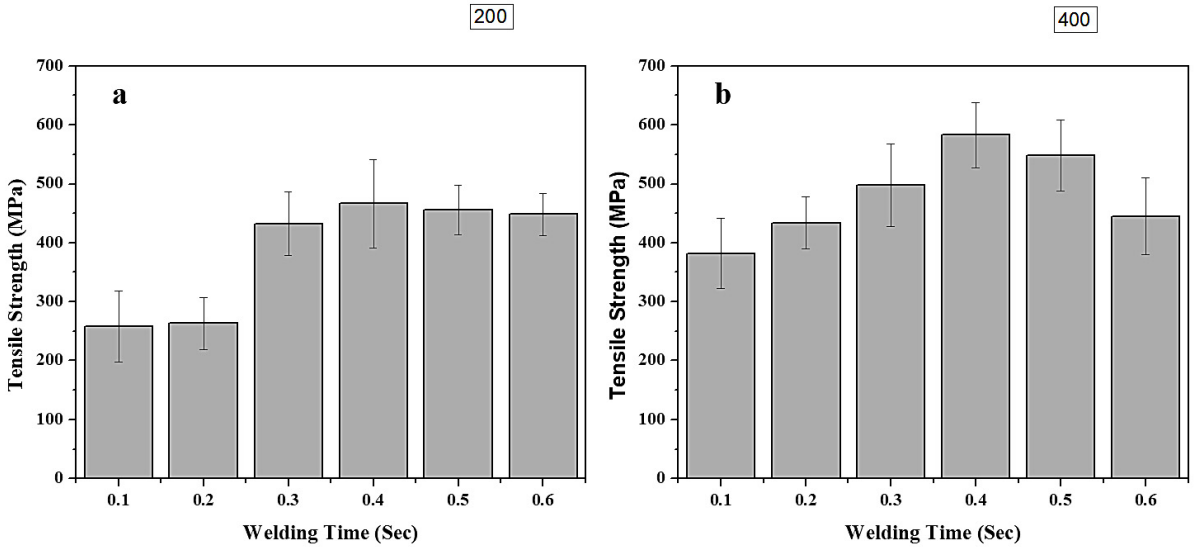

Fig. 3. Tensile strength of the samples processed at a) 20 0A welding current, and b) 400 A welding current with different welding time, error bars are the standard deviation of the 3 measurements

tensile strength increased with welding time up to 0.4 s to reach 538 MPa, as the welding time increased above 0.4 s at constant welding current (400 A), the tensile strength decreased. This is probably attributed to the grain growth due to high heat input to the welding area. In the other word, the maximum tensile strength of 538 MPa was recorded with sample performed with 400 A welding current and 0.4 welding time.

A similar result was reported by Hameed et al. [23], which they performed bending test of AISI 304 screw stud using arc stud welding. The successful results were obtained for current and time values (400 A, 0.25 sec), (600 A, 0.3

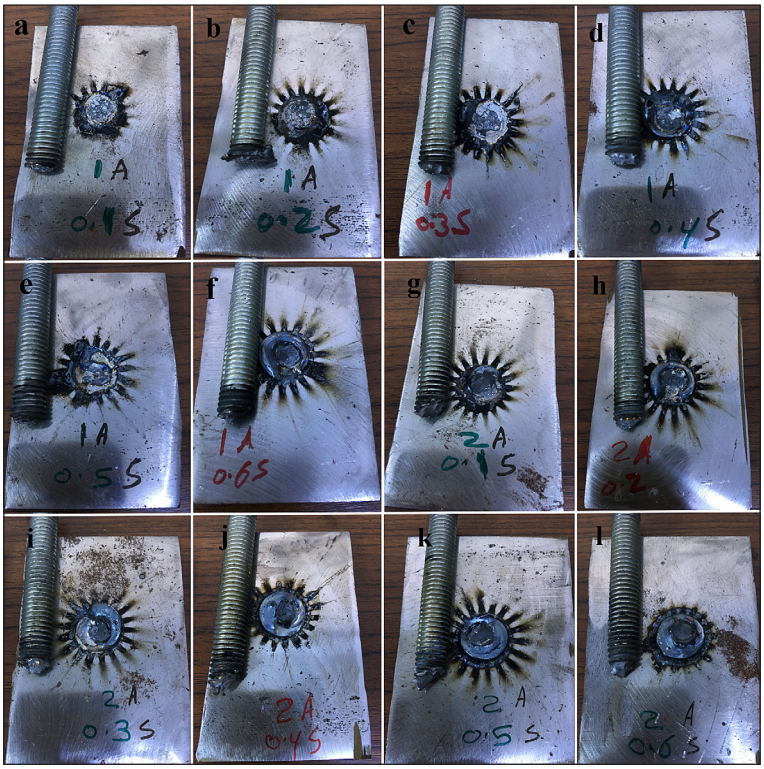

Fig. 4. The fracture mode of the arc stud welding as a function of increasing welding current and time a-f) at 200A welding current with 0.1, 0.2, 0.3, 0.4, 0.5, 0.6 s welding time, respectively, and g-i) at 400A welding current with 0.1, 0.2, 0.3, 0.4, 0.5, 0.6 s welding time, respectively

sec), and (800 A, 0.25 sec). The present results record optimum combinations (200 A, 0.4 sec) and (400 A, 0.4 sec). The current work recorded optimal values for the current less than that of Hameeds' research because the current stud is for low carbon steel and needs less current than the stainless steel stud used for them.

Figure 4 presents the fracture mode of the arc stud welding as a function of increasing of welding current and time. Three main failure modes were observed during the tensile test, the first mode is interface fracture, in this mode the fracture propagates between the stud and substrate surface results of incomplete melting and alloying of both stud and substrate at low processing parameter (200A welding current, 0.1 and 0.2 s welding time), Figures 4 a,b. The second failure is pullout fracture which is distinguished by a hole in the substrate surface figure c-i at processing condition of constant welding current of 200 A welding current with 0.3, 0.4, 0.5 and 0.6 s welding time for Figure 4 c-f, and 400 A current with 0.1, 0.2 and 0.3 s, for Figure 4 g-i, respectively. The last failure mode occurs in the stud shank instead of the weldment interface or heat affected zone Figure 4 j-l [3], at processing condition of 400 A welding current with 0.4, 0.5 and 0.6 s welding time, respectively.

The joint performed using welding current of 400 A and welding time 0.4 s shows a highest mean tensile strength of 583 MPa which is considered as a preferred process parameter. Figure 5 presents tensile strength and failure mode of five joints, one joint is prepared with preferred parameters (400 A and 0.4 s welding current and time, respectively), two joints prepared with 0.1 and 1 gram of SiC particles and preferred parameters, another two joints

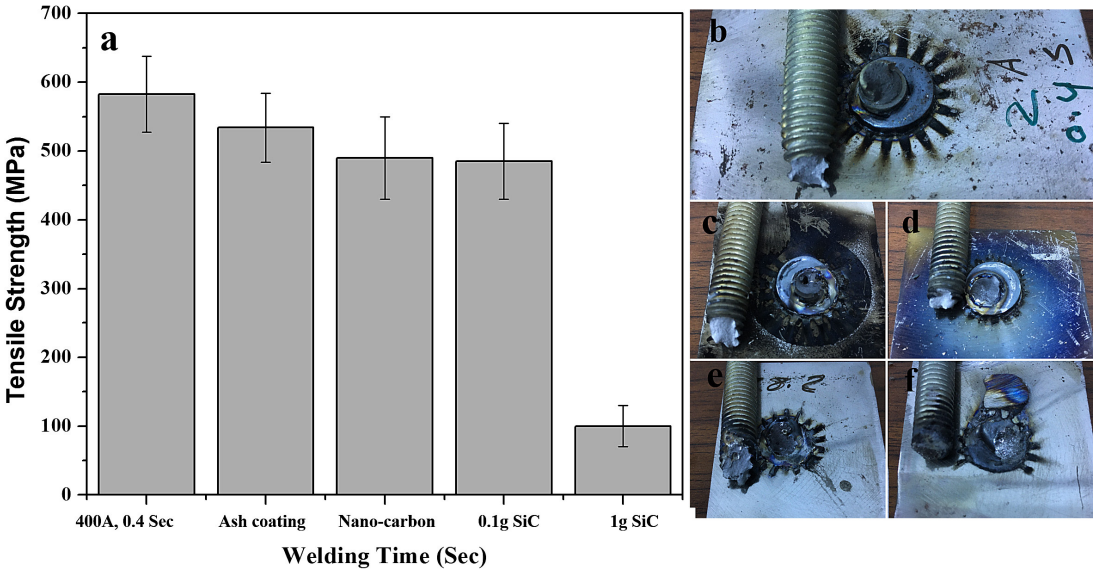

Fig. 5. a) tensile strength, and failure mode of stud welding, of b) preferred parameters 400 A, 0.4 s c) ash coating d) carbon nano coating e) adding 0.1 gram SiC and f) adding 1 gram SiC

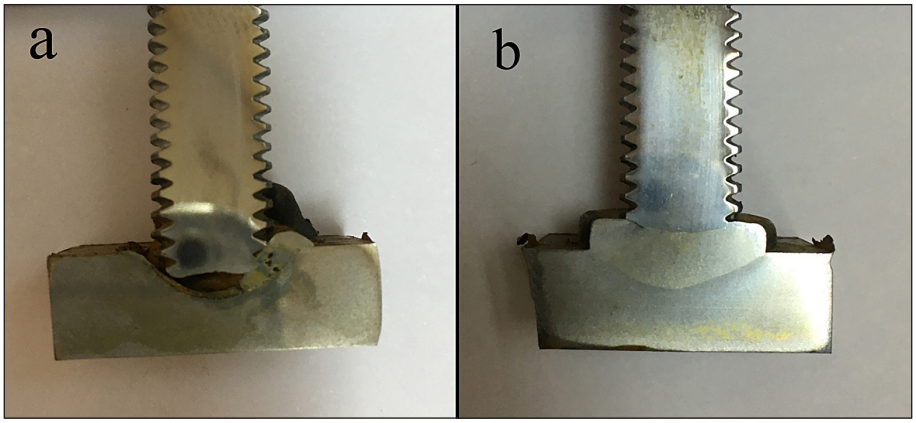

Fig. 6. fracture mode of the arc stud welding preferred parameters 400 A, 0.4 s a) with adding 1 gram SiC b) without adding 1 gram SiC

prepared with substrate coated with carbon Nano-layer and ash at preferred parameters. The tensile strength slightly reduced of the joints fabricated with ash and nano carbon coated substrate.

Similarly, adding of 0.1 SiC particles to the welding area led to a small reduction in tensile strength. However, increase the SiC weight to 1 gram resulted in sharp reduction in tensile strength. This is probably can be attributed to form unstable arc which led to incomplete melting Figure 6a. Again, joint prepared using performed welding current of 400 A and welding time 0.4 s shows a uniform distribution of materials with almost free of defect Figure 6b.

Microstructure and microhardness

Figure 7 presents the cross section and selected microstructure region of the arc stud welding joint prepared at 400 A welding current and 0.4 s welding time. Figure 7b shows the microstructure of the AISI 1106 stud. It is consisting of equiaxed grains of ferrite (bright grain), with small amount of pearlite (dark grain) [24, 25]. Figure 7c, presents the heat affected zone HAZ of the welded sample of the low carbon steel side of the fusion zone (stud), it is characterized by recrystallisation and fine grains with increase the amount of pearlite and the presence of some martensite due to high cooling rate. Figure 7e showed the HAZ of the welded sample of the medium carbon steel side of the fusion zone (plate), this zone is characterized by fine grains with high amount of perlite, a micro cracks and micro voids at the FZ/HAZ may also appear [26, 27], which may be attributed to the increase carbon percentage at the medium carbon steel side. The fusion zone consists of re-solidified with very fine grain of mixed of ferrite and perlite Figure 7d [3], A micro voids is also presented in the fusion zone. Figure 7f shows the microstructure of the AISI 1045 plate, which consists mainly of pearlite in a matrix of ferrite [28].

Figure 8 shows the hardness of the stud (low carbon steel), medium carbon steel and the fusion zone of the weld joint produced at 400 A current and 0.4 s welding time.

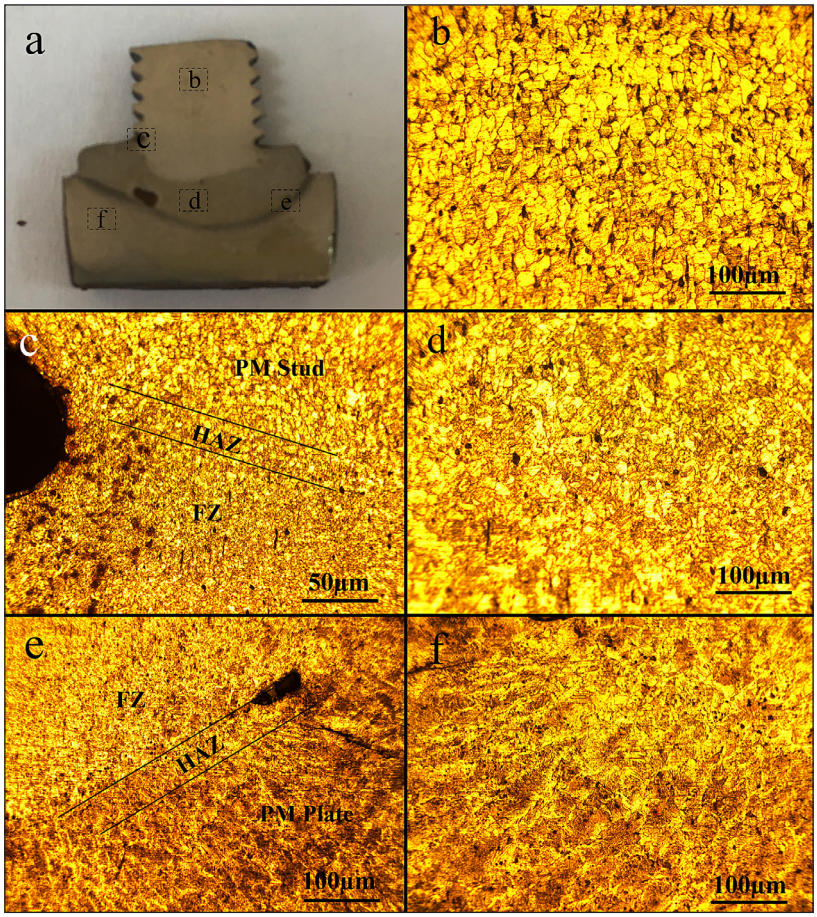

Fig. 7. a) Cross section of arc stud welding preferred parameters 400 A, 0.4 s, and microstructure of d) AISI 1106 stud, c) heat affected zone HAZ of the welded sample of stud side, d) fusion zone, e) heat affected zone HAZ of the welded sample of plate side and f) AISI 1045 plate

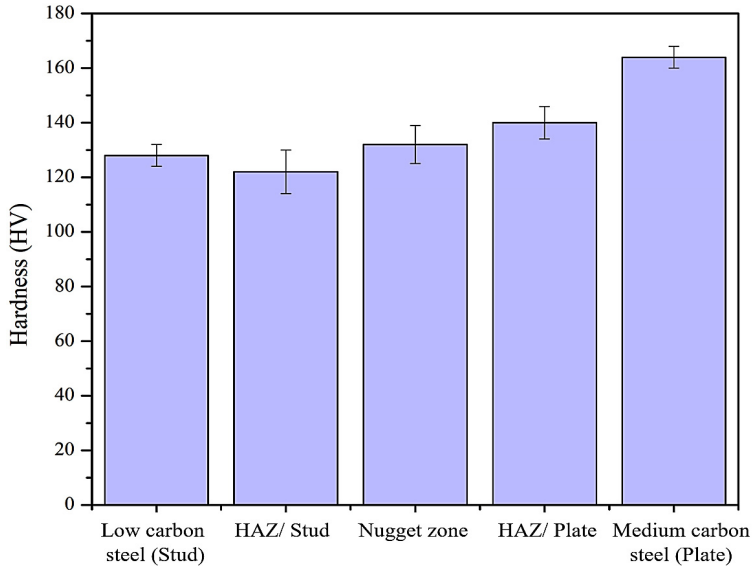

Fig. 8. Microhardness of arc stud welding prepared at preferred parameters 400 A, 0.4 sec

The hardness of the parent metals was recorded of 128 HV and 164 HV for the stud and plate, respectively. The hardness of the fusion zone was 132 HV which it slightly higher than the hardness of the stud, this is probably attributed to the grain refinement and present the perlite. The hardness of HAZ at plate side was 140 HV which it higher than that of the fusion zone due to the high amount of carbon and consequently high amount of perlite as shown in Figure 7c.

CONCLUSIONS

The arc stud welding process is successfully employed for joining fully threaded low carbon steel stud with 10 mm diameter and 8 cm length to 8 mm medium carbon steel plate. The influence of processing parameter including welding current 200, 400 A and welding time 0.1–0.6 s with the effects of adding SiC and applying carbon nano layer to welding area was investigated. The main conclusions in the present study are the following:

1. The maximum tensile strength of 583 MPa was obtained at 400 A and 0.4 s welding current and welding time.
2. Three failure modes were obtained during tensile test which are interface fracture between stud and plate surface because of incomplete melting at low processing parameters of 200 A and 0.1, 0.2 s, current and welding time, respectively. The second failure mode is pull-out fracture which is featured by a hole in the workpiece plate surface. The last failure mode occurs in the threaded stud shank instead of the weldment interface or heat affected zone.
3. The microstructure of the fusion zone is characterized by fine grains of ferrite and perlite, a micro cracks with micro voids at the FZ / HAZ may also appear.
4. The microhardness at the fusion zone of the stud welded joint was recorded of 132 HV which it slightly higher than the stud hardness 128 HV and lower than that of the plate of 164 HV.

REFERENCES

1. Chambers, H.A. 2001. Principles and practices of stud welding. Pci Journal, 46(5), pp. 46–59.
2. Samardžić, I., Kolumbić, Z. and Klarić, Š. 2009. Welding parameter monitoring during stud arc welding. Pollack Periodica, 4(1), pp. 29–39. https://doi.org/10.1556/pollack.4.2009.1.4
3. Abass, M.H., Abood, A.N., Alali, M., Hussein, S.K. and Nawi, S.A. 2021. Mechanical Properties And Microstructure Evolution in Arc Stud Welding Joints of AISI 1020 with AISI 316L and AISI 304. Metallography, Microstructure, and Analysis, 10(3), 321–333. https://doi.org/10.1007/s13632-021-00744-8
4. Magda, A., Burca, M. and Lego, M. 2018, September. Research regarding capacitor discharge stud welding with tip ignition on galvanized thin sheets. In: IOP Conference Series: Materials Science and Engineering, 416, 1, #012015. DOI 10.1088/1757-899X/416/1/012015
5. Behrens, B.A., Gruß, D. and Jenicek, A. 2011. Stud welding within sheet metal working tools. Production Engineering, 5(3), pp. 283–292. https://doi.org/10.1007/s11740-011-0304-3
6. Brätz, O. and Henkel, K.M. 2019. Investigation of

diffusible hydrogen content in drawn arc stud weld metal. Welding in the World, 63(4), pp. 957–965. https://doi.org/10.1007/s40194-019-00730-3

7. Hildebrand, J. and Soltanzadeh, H. 2014. A review on assessment of fatigue strength in welded studs. International Journal of Steel Structures, 14(2), pp. 421–438. https://doi.org/10.1007/s13296-014-2020-2
8. Nishikawa, W.A.I.C.H.I. 2003. The principle and application field of stud welding. Welding international, 17(9), pp .699–705. https://doi.org/10.1533/wint.2003.3170
9. Hartz-Behrend, K., Marqués, J.L., Forster, G., Jenicek, A., Müller, M., Cramer, H., Jilg, A., Soyer, H. and Schein, J. 2014, November. Stud arc welding in a magnetic field–Investigation of the influences on the arc motion. In: Journal of Physics: Conference Series, 550, 1, #012003. https://iopscience.iop.org/article/10.1088/1742-6596/550/1/012003/meta
10. Klaric, S., Kladaric, I., Kozak, D., Stoic, A., Ivandic, Z. and Samardzic, I. 2009. The influence of the stud arc welding process parameters on the weld penetration. Scientific Bulletin Series C: Fascicle Mechanics, Tribology, Machine Manufacturing Technology, 23, p. 79.
11. Yilmaz, N.F. and Hamza, A.A. 2014. Effect of process parameters on mechanical and microstructural properties of arc stud welds. Materials Testing, 56(10), pp. 806–811. https://doi.org/10.3139/120.110629
12. Hsu, C. and Mumaw, J. 2011. Weldability of advanced high-strength steel drawn arc stud welding. Welding journal, 90, pp. 45–53.
13. Zhang, Q., Zhang, B., Luo, Y., Yang, G. and Zheng, H.X. 2022. Effect of the Welding Process on Microstructure, Microhardness, and Residual Stresses of Capacitor Discharge Stud Welded Joint. Journal of Manufacturing Science and Engineering, 144(1). https://doi.org/10.1115/1.4051533
14. Singh, D.K., Sahoo, G., Basu, R., Sharma, V. and Mohtadi-Bonab, M.A. 2018. Investigation on the microstructure – mechanical property correlation in dissimilar steel welds of stainless steel SS 304 and medium carbon steel EN 8. Journal of Manufacturing Processes, 36, pp. 281–292. https://doi.org/10.1016/j.jmapro.2018.10.018
15. Jafarzadegan, M., Feng, A.H., Abdollah-Zadeh, A., Saeid, T., Shen, J. and Assadi, H. 2012. Microstructural characterization in dissimilar friction stir welding between 304 stainless steel and st37 steel. Materials Characterization, 74, pp. 28–41. https://doi.org/10.1016/j.matchar.2012.09.004
16. Abbas, E.N., Omran, S., Alali, M., Abass, M.H. and Abood, A.N. 2018, October. Dissimilar welding of AISI 309 stainless steel to AISI 1020 carbon steel using arc stud welding. In: International Conference on Advanced Science and Engineering, pp. 462–467. https://doi.org/10.1109/ICOASE.2018.8548844
17. Başyiğit, A.B. and Kurt, A. 2017. Investigation of the weld properties of dissimilar S32205 duplex stainless steel with AISI 304 steel joints produced by arc stud welding. Metals, 7(3), p. 77. https://doi.org/10.3390/met7030077
18. Buranapunviwat, K. and Sojiphan, K. 2021. Destructive testing and hardness measurement of resistance stud welded joints of ASTM A36 steel. Materials Today: Proceedings, 47, pp.3 565–3569. https://doi.org/10.1016/j.matpr.2021.03.562
19. Lin, Y.C., Chen, H.M. and Chen, Y.C. 2013. Analysis of microstructure and wear performance of SiC clad layer on SKD61 die steel after gas tungsten arc welding. Materials and Design, 47, pp. 828–835. https://doi.org/10.1016/j.matdes.2013.01.007
20. Moradi, M.M., Jamshidi Aval, H. and Jamaati, R. 2018. Microstructure and mechanical properties in nano and microscale SiC-included dissimilar friction stir welding of AA6061-AA2024. Materials Science and Technology, 34(4), pp. 388–401. https://doi.org/10.1080/02670836.2017.1393976
21. Xie, X., Shen, J., Cheng, L., Li, Y. and Pu, Y. 2015. Effects of nano-particles strengthening activating flux on the microstructures and mechanical properties of TIG welded AZ31 magnesium alloy joints. Materials & Design, 81, pp. 31–38. https://doi.org/10.1016/j.matdes.2015.05.024
22. ISO 14555, (2006). In Welding-Arc Stud Welding of Metallic Materials, 2nd ed. Geneva, Switzerland.
23. Firas H. Hameed, et al. Dissimilar arc stud welding AISI 304/ AISI 1008: Mechanical properties. In: IOP Conf. Series: Materials Science and Engineering 1076 (2021) 012079. https://iopscience.iop.org/article/10.1088/1757-899X/1076/1/012079/meta
24. Algodi, Samer J., et al. Modelling and characterisation of electrical discharge TiC-Fe cermet coatings. Procedia CIRP 68 (2018): 28–33. https://doi.org/10.1016/j.procir.2017.12.017
25. Shin, Dong Hyuk, et al. Microstructural evolution in a commercial low carbon steel by equal channel angular pressing. Acta Materialia 48.9 (2000): 2247–2255. https://doi.org/10.1016/S1359-6454(00)00028-8
26. Ma, H., Qin, G., Geng, P., Li, F., Fu, B. and Meng, X. 2015. Microstructure characterization and properties of carbon steel to stainless steel dissimilar metal joint made by friction welding. Materials & Design, 86, pp. 587–597. https://doi.org/10.1016/j.matdes.2015.07.068
27. Khan, M., Dewan, M.W. and Sarkar, M.Z. 2021. Effects of welding technique, filler metal and post-weld heat treatment on stainless steel and mild steel dissimilar welding joint. Journal of Manufacturing Processes, 64, pp. 1307-1321. https://doi.org/10.1016/j.jmapro.2021.02.058
28. Kuroiwa, Ryosuke, et al. 2019. Microstructure control of medium carbon steel joints by low-temperature linear friction welding. Science and Technology of Welding and Joining. https://doi.org/10.1080/13621718.2019.1600771